EFFECTS OF CRACK MORPHOLOGY AND CLOSURE ON ULTRASONIC RESPONSE

R. A. Roberts

Citation: AIP Conf. Proc. **1096**, 1434 (2009); doi: 10.1063/1.3114125
View online: http://dx.doi.org/10.1063/1.3114125
View Table of Contents: http://proceedings.aip.org/dbt/dbt.jsp?KEY=APCPCS&Volume=1096&Issue=1
Published by the American Institute of Physics.

EFFECTS OF CRACK MORPHOLOGY AND CLOSURE ON ULTRASONIC RESPONSE

R. A. Roberts
Center for NDE, Iowa State University, Ames, IA 50014

ABSTRACT. Progress is reported on the development of tools for the study of the influence of crack morphology and closure on ultrasonic inspection response. An in-situ phased array sector scan is described for the monitoring of crack responses under load, and results are presented showing the anticipated dependence of signal amplitude on crack closure. Acoustic microscopy mapping of actual crack morphology is outlined. A measurement model is presented for prediction of responses using the measured crack morphology as input. Results are shown demonstrating the reduction in inspection signal amplitude arising from the deviation of measured crack morphology from the ideal planar geometry.

Keywords: Ultrasonics, Crack Morphology
PACS: 43.35.Yb 43.35.Zc 43.38.Hz

INTRODUCTION

Inspection sensitivity is most often quantified as the response to a reflector having a canonical geometry such as a flat bottomed hole or EDM notch. It is well understood that the reflectivity of an actual flaw can vary substantially from that of a canonical reflector of comparable size. This variation is in large part due to differing flaw morphologies. Additionally, in the case of cracks, signal variability can also arise from crack closure, where large compressive stress hold the crack faces in intimate physical contact, thereby allowing the transmission of energy through the crack faces, and consequently reducing flaw signal amplitude. A program is ongoing at CNDE to examine the effects of flaw morphology and crack closure on NDE inspection, with primary emphasis on eddy current and X-Ray inspection modalities. An auxiliary effort is included to examine specimens ultrasonically as they are processed. This paper summarizes the tools that have been assembled for the ultrasonic activity, and presents preliminary results indicating the sensitivity of the ultrasonic measurement to flaw morphology and crack closure.

IN-SITU ULTRASONIC MEASUREMENT

A task is being pursued addressing the in-situ monitoring of fatigue crack growth in four point bending using eddy current sensors.[1] A complementary ultrasonic measurement was sought to allow simultaneous ultrasonic monitoring, without disrupting the eddy current instrumentation. The measurement configured for this purpose is shown in Fig.(1). An ultrasound beam is electronically swept over the vicinity of the crack using a 10 MHz phased array transducer arranged to generate a shear wave with transmission angles ranging from approximately 60 to 70 degrees. The array has rectangular aperture dimensions of 10 mm in the active direction, and 7 mm in the passive direction. The active

CP1096, *Review of Quantitative Nondestructive Evaluation Vol. 28,*
edited by D. O. Thompson and D. E. Chimenti

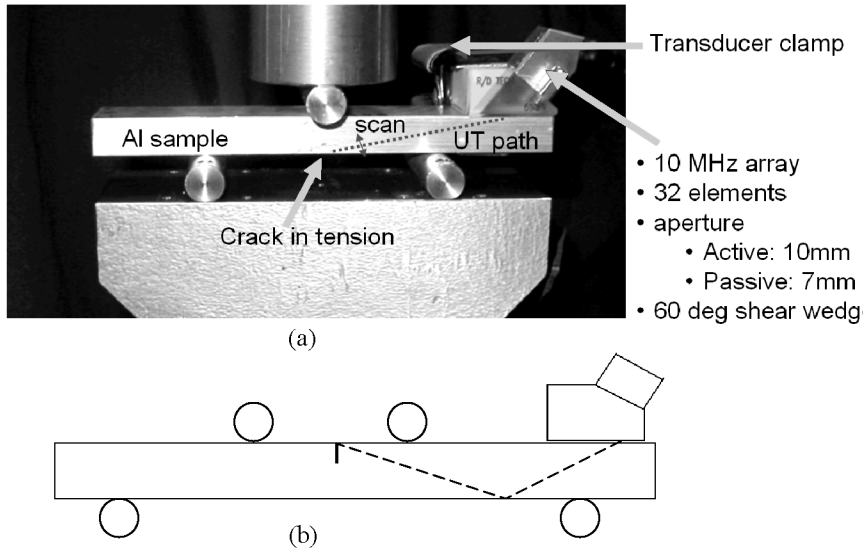

FIGURE 1. Ultrasonic phased array measurement for in-situ monitoring of fatigue crack under load. (a) crack in tension, (b) crack in compression.

direction is divided into 32 elements. The array is coupled to the specimen through a 60 degree shear wedge. The specimens are aluminum bars having dimensions of 6 inch x 1 inch x 0.5 inch. The array transducer is positioned at the end of the specimen, so as to be out of the way of bending rollers and eddy current sensors attached in the immediate vicinity of the crack. The positioning of the transducer is shown in Fig.(1) for 3 point bending. The same positioning is used for four point bending. The arrangement shown in Fig.(1a) is used for monitoring responses when the crack is loaded in tension. To load the crack in compression, the specimen is turned upside down in the fixture, as shown in Fig.(1b). In this case, the crack is accessed ultrasonically through a reflection from the bottom surface of the specimen.

SIGNAL DEPENDENCE ON CRACK CLOSURE

Measurements were taken in-situ using the configuration of Fig.(1) on a number of fatigue crack specimens, under states of compression and tension. Data was collected with loads varying from 0% to 80% of yield. Results are shown in Fig.(2) for one such specimen which demonstrate the anticipated response to loading. In the sector scans of Fig.(2a), the signal from the crack in tension arrives at an earlier time and greater angle than when the sample is oriented to place the crack in compression, due to the differences in propagation paths as depicted in Fig.(1). Individual signals selected from the sector scans (indicated by the horizontal lines drawn through the sector scans) are plotted as a function of load in Fig.(2b), where load is expressed as percent of yield. The expected decrease in signal amplitude is observed when the crack is placed in compression. Little change is seen in the response amplitude when placed in tension. In both cases, small changes are seen in the signal structure due to the physical deformation of the specimen, resulting in a shortening (when in compression) or lengthening (when in tension) of the propagation path, and corresponding slight change in propagation angles.

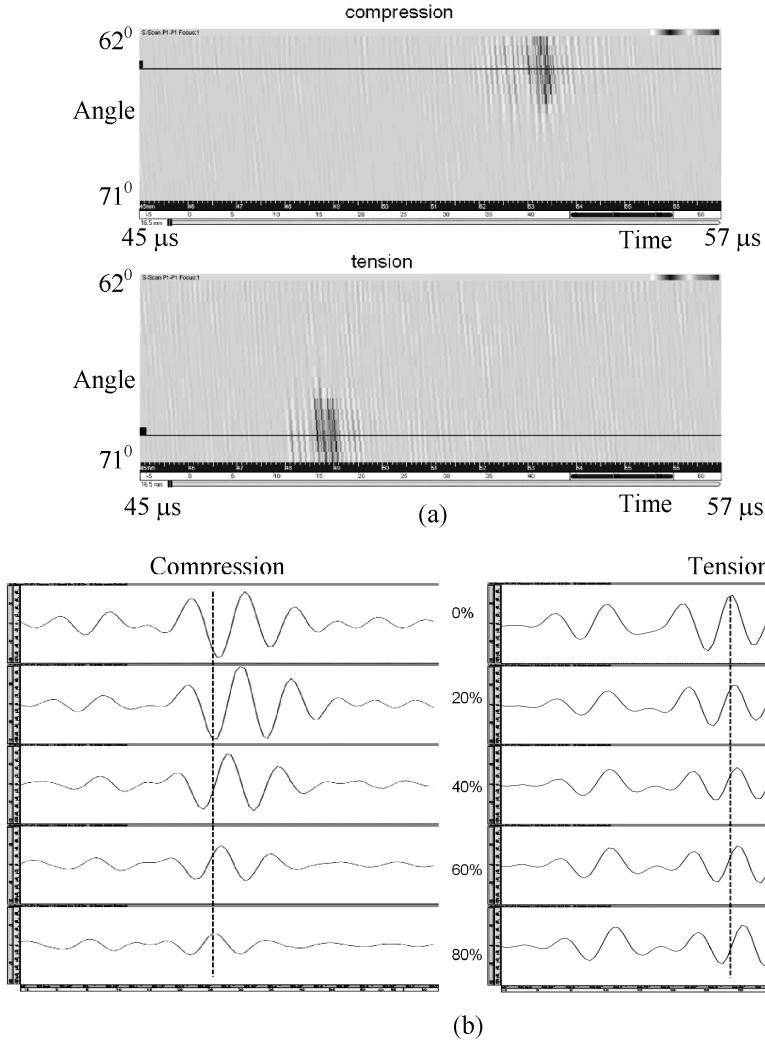

FIGURE 2. Ultrasonic response of fatigue crack under loading. (a) Phased array sector scans for a crack under compression and tension. (b) Crack signals as function of load under compression and tension (% yield).

MEASUREMENT MODEL FOR PREDICTION OF MORPHOLOGY EFFECTS

A computational model was implemented for the ultrasonic measurement described in the preceding section. The model consists of two components: 1) a model for the propagation of the ultrasonic beam generated by the wedge-mounted array transducer into the aluminum bar specimen, and 2) a model for computing the response to the presence of the crack. The ultrasonic beam model exploits the Cartesian nature of the bar geometry through Fourier transformation of the wave fields in the x_1, x_2 dimensions of the bar, as depicted in Fig.(3). The time harmonic displacement field in the bar is thereby expressed in the form

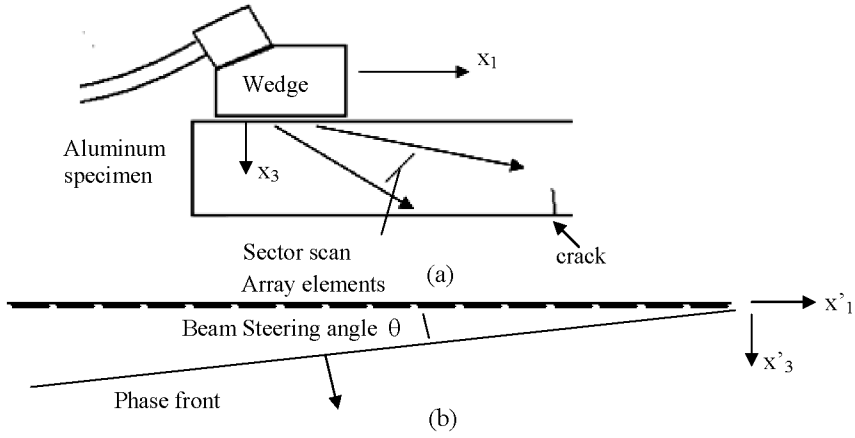

FIGURE 3. Geometry guiding the measurement model: a) transducer/wedge assembly on specimen, b) local geometry of array transducer elements.

$$u_i(x_1,x_2,x_3,\omega) = \iint f(k_1,k_2,\omega)\ (\ \ T_i^{\alpha}(k_1,k_2,\omega)\exp(i\,k_3^{\alpha}\,(x_3 - x_3^{ts})) + T^{\alpha}(k_1,k_2,\omega)\,R_i^{\beta}(k_1,k_2,\omega)\exp(-i\,k_3^{\beta}\,(x_3 - x_3^{bs}))\ \ )\exp(i\,k_1\,x_1 + i\,k_2\,x_2)\,dk_1\,dk_2 \quad (1)$$

where k_1, k_2 are spatial frequency variables associated with the x_1, x_2 directions, and ω is time harmonic frequency. In this formulation, the ultrasonic wedge is viewed as a half-space from which an ultrasonic beam emerges, where the ultrasonic beam is prescribed by its spatial frequency spectrum $f(k_1,k_2,\omega)$. The spatial frequency spectrum is evaluated for the array transducer as

$$f(k'_1,k'_2,\omega) = \frac{\Delta_1\,\Delta_2}{4\,\pi^2}\,\mathrm{sinc}(k'_1\,\Delta_1/2)\,\mathrm{sinc}(k'_2\,\Delta_2/2)\sum_{n=1}^{32}\exp(i\,(\omega/c_w\ \sin(\theta) - k'_1)\,x'_{1n}) \quad (2)$$

where k_1', k_2' are Fourier transform variables in the x'_1, x'_2 plane containing the array elements, Δ_1 and Δ_2 are the element dimensions in the x'_1, x'_2 directions, with elements centered at positions x'_{1n}, θ is the angle at which it is desired to steer the beam, and c_w is the wave velocity in the wedge. When used in Eq.(1), a coordinate transformation is applied from the local k_1', k_2' coordinates of the array to the k_1, k_2 coordinates of the measurement model.

The beam is transmitted through the top interface $x_3 = x_3^{ts}$ with the displacement transmission coefficient $T_i^{\alpha}(k_1,k_2,\omega)$. The beam is reflected from the bottom surface $x_3 = x_3^{bs}$ with displacement reflection coefficient $R_i^{\beta}(k_1,k_2,\omega)$, where $T^{\alpha}(k_1,k_2,\omega)$ is the scalar potential transmission coefficient at the top interface. The transmission and reflection coefficients in Eq.(1) can be prescribed as for either compressional (α,β=L) or shear (α,β=T) waves, and these coefficients can extend beyond the range of propagating energy, thereby representing non-propagating near surface phenomena, such as surface creeping waves. The wave field is non-propagating at spatial frequencies for which the normal wave vector component

$$k_3^{\alpha} = (\omega^2/c_{\alpha}^2 - k_1^2 - k_2^2)^{1/2} \quad (3)$$

is imaginary, where c_{α} is wave velocity.

The scheme for evaluating the integral in Eq.(1) treats the integration in polar coordinates, with radial and angular variables k_r and ν replacing Cartesian variables k_1, k_2. It is noted that the integrand displays a simple behavior dominated by a single stationary phase point in the angular variable ν. This integration is therefore evaluated using a straightforward stationary phase analysis. In contrast, the integrand displays quite complex non-analytic behaviors in the radial variable, corresponding to the various interface-related transmission and reflection phenomena. The integration is carried out numerically in this variable, following a deformed integration contour in the complex k_r plane which circumvents points of non-analytic behavior.

The signal due to the presence of the crack is evaluated using Auld's reciprocity integral evaluated over the face of the crack [2]

$$v(\omega) = E(\omega) \int_{crack} u_i^{tot}(x,\omega)\, \tau_{ij}^{inc}(x,\omega)\, n_j\, dx \tag{4}$$

where $E(\omega)$ is a frequency dependent coefficient describing, among other things, the bandpass characteristics of the transducer and instrumentation, $u^{tot}_i(x,\omega)$ is the total displacement field on the face of the crack, and $\tau^{inc}_{ij}(x,\omega)\, n_j$ is the normal traction over the surface determined by the crack face geometry, that would exist in the absence of the crack, i.e., the "incident field" determined using the beam model described above. The exact determination of the total displacement field on the face of the crack is an extremely challenging problem. Approximations are employed to provide a useful model based on Kirchhoff scattering theory. In this procedure, the displacement at some position on the crack face is computed as if the incident field were reflecting from a plane surface tangent to the crack face at that position. The displacement so computed is then summed over the face of the crack in accordance with the integration indicated by Eq.(4). It is understood that such an approach with underestimate the strength of signals diffracted by the crack edges. The model has the capability to correct the strength of edge-diffracted signals using edge diffraction theory as described in [3]. It was observed in the applications considered in the present work, however, that the received signals are dominated by strong specularly reflected signals, making the edge diffraction corrections unnecessary. Spectral components of the response are evaluated individually, then Fourier transformed in ω to obtain time domain responses.

When considering the case of cracks in compression, as depicted in Fig.(1b), the reflection from the bottom surface used to gain access to the crack is treated as a perfect reflection, i.e. as if the signal were propagating without reflection to a mirror-symmetric geometric configuration below the reflecting interface. This simplification is justified by the fact that only shear wave reflections well beyond the L-wave critical angle are being considered.

ACOUSTIC MICROSCOPY MEASUREMENT OF CRACK MORPHOLOGY

Study of the effects of real-world crack morphology on inspection signals requires a means to determine real world crack morphologies. The work reported here is pursuing the use of high frequency acoustic microscopy to perform this determination. The crack contained in a selected specimen was isolated through sectioning within a smaller specimen appropriate for acoustic microscopy examination. The specimen was sectioned so that the fatigue crack is centered approximately parallel to the faces of a 0.25 inch slice of the specimen, as depicted in Fig.(4a). The crack was examined using a 100 MHz, 0.25 in. dia., 1.0 in. F.L. transducer, capable of focusing to a 0.25 inch depth in the aluminum specimen. Pulse-echo data was collected over the face of the crack using a 20 micron pixel. The

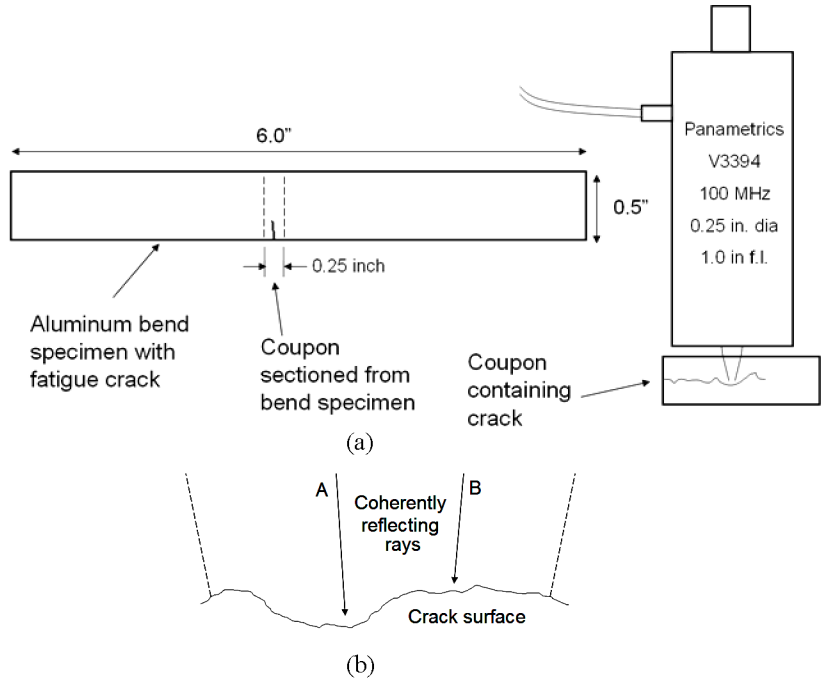

FIGURE 4. Acoustic microscopy of sectioned fatigue crack: a) coupon sectioning, b) beam interaction with multiple reflecting features on crack face.

conversion of signal arrival times into distance to the crack face required development of data processing capable of accommodating the complexity of the reflecting surface morphology. At certain pixel positions, multiple return signals were observed, corresponding to multiple morphological features falling within the diameter of the ultrasonic beam. Figure (4b) depicts such a case, in which two ray paths providing coherent reflected signals are identified, each arriving at a different time. An approach was developed based upon viewing the envelope of the pulse-echo signal as a probability function, from which the position of the crack face at the center of the beam is evaluated as the expectation. This approach enabled a simple robust mapping of complex signals onto surface positions, and was observed to provide realistic-looking continuous transitions between neighboring unambiguous morphological features. The mapping of the crack geometry obtained with this approach is shown in Fig.(5). Figure (5a) presents a 3D shaded surface drawing of the extracted geometry. A more quantitative indication of the surface morphology is seen in the line profile of Fig.(5b).

INFLUENCE OF CRACK MORPHOLOGY ON INSPECTION SIGNAL

The measured crack geometry obtained by acoustic microscopy was used in the measurement model to examine the effect of the non-deal crack morphology on the inspection measurement depicted in Fig.(1). The crack geometry shown in Fig.(5) was used as the surface of integration in evaluating Eq.(4), where the incident traction field $\tau^{inc}_{ij}(x,\omega)\ n_j$ is evaluated using the beam transmission model as expressed by Eq.(1). The

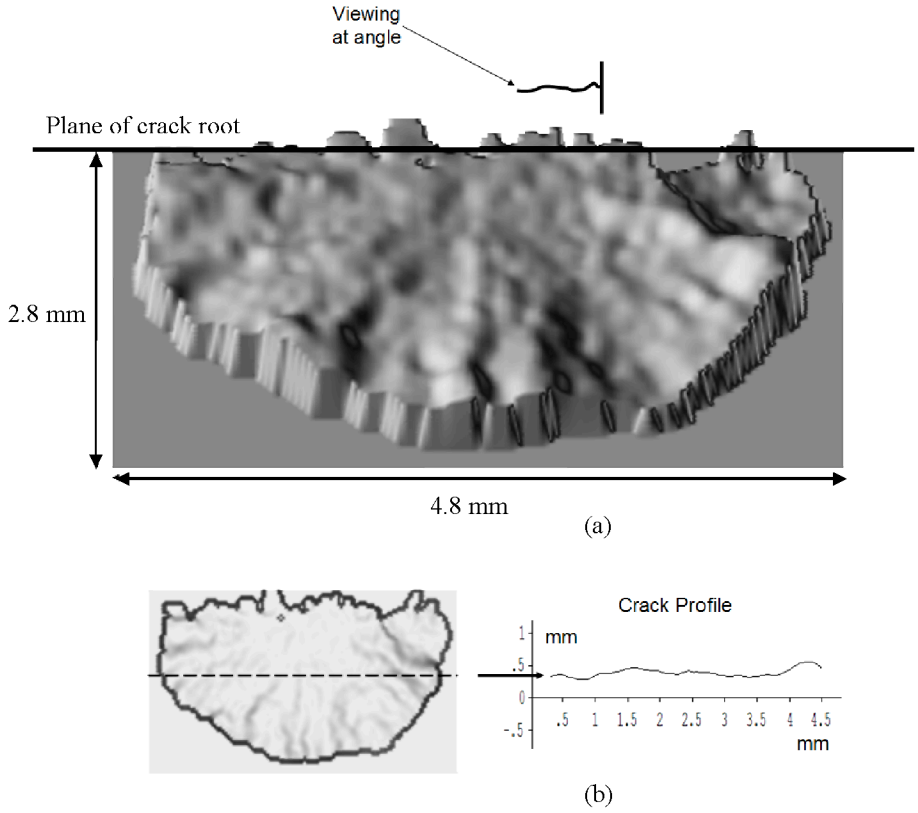

FIGURE 5. Acoustic microscopy mapping of crack face: (a) shaded surface drawing (b) line profile through center of crack..

computation considered transmission to shear waves at the top interface in Fig(3a), and the reflection into compressional and shear waves at the bottom surface. Although the compressional wave is non-propagating at the reflection angles considered, a small contribution from the interaction of this wave field with the crack is observed, and is therefore included. The total displacement $u^{tot}_i(x,\omega)$ at points on the measured the crack surface was evaluated using a Kirchhoff-based analysis, as previously discussed.

It was observed that the dominant contributions to the response signal were due to near-specular reflections from the crack face. These consist of signals which first reflect from the crack face, followed by reflection from the bottom surface, then return to the transducer, or vice-versa. In the case of an ideal flat crack oriented perpendicular to the bottom surface, these reflections display a strong coherence (perfectly specular for plane wave incidence), thereby yielding strong signals. The question of interest is the extent to which this coherence will be disrupted by deviations from the ideal planar crack geometry. Results of the numerical evaluation of Eq.(4) are shown in Fig.(6) when using the measured crack geometry depicted in Fig.(5). These results are compared to the results obtained when using a comparably sized crack having an ideal planar geometry. It is seen that the loss of coherence in the near-specular reflections from the irregularly shaped crack face result in a substantial 8.3 dB loss of signal amplitude.

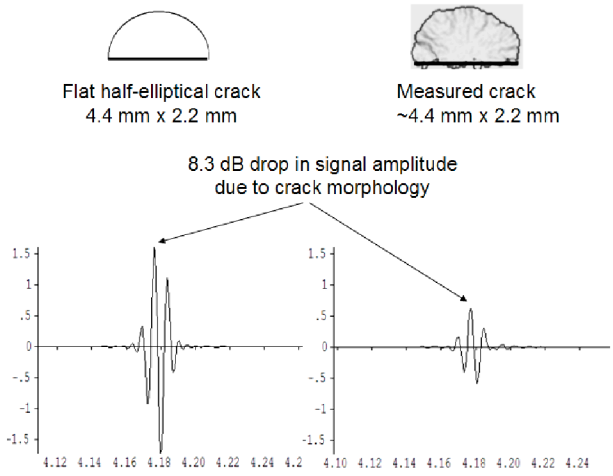

FIGURE 6. Model prediction of signal loss due to measured crack morphology in Fig.(5).

SUMMARY

A set of tools has been developed for the examination of the effect of crack morphology and closure on ultrasonic inspection signals. A scanned phased array measurement allows in-situ monitoring of fatigue crack specimens under load. Acoustic microscopy techniques provide a direct measurement of crack morphology, which can be used in a computational model of the phased array measurement to predict the effect of measured morphology on the inspection response. Upcoming work will use these tools to examine the response of numerous crack specimens as they are produced in the on-going study of the effects of crack morphology. This work will include benchmark comparisons of machined reflectors versus grown fatigue cracks to validate model predictions.

ACKNOWLEDGEMENT

This material is based upon work supported by the Air Force Research Laboratory under Contract # FA8650-04-C-5228 at Iowa State University's Center for NDE.

REFERENCES

1. C.C.H. Lo and N. Nakagawa, "Effects of Dynamic and Static Loading on Eddy Current NDE of Fatigue Cracks," *these Proceedings*.
2. B. Auld, "General Electromechanical Reciprocity Relations Applied to the Calculation of Elastic Wave Scattering Coefficients," Wave Motion Vol. 1, 1979.
3. R. Roberts, "Recent Developments in Kirchhoff Crack Tip Diffraction Corrections," Proceedings Review of Progress in Quantitative Nondestructive Evaluation Vol. 18, D.O. Thompson and D.E. Chimenti, Eds., AIP, N.Y., 1999.